# Linear GPR Imaging Based on Electromagnetic Plane-Wave Spectra and Diffraction Tomography

**Meincke, Peter**

*Published in:*
Tenth International Conference on Ground Penetrating Radar

*Publication date:*
2004

*Document Version*
Publisher's PDF, also known as Version of record

# Linear GPR Imaging Based on Electromagnetic Plane-Wave Spectra and Diffraction Tomography

Peter Meincke
Ørsted·DTU, Electromagnetic Systems
Technical University of Denmark
Ørsteds Plads, Building 348
DK-2800 Kgs. Lyngby, Denmark
Email: pme@oersted.dtu.dk

*Abstract*— **Two linear diffraction-tomography based inversion schemes, referred to as the Fourier transform method (FTM) and the far-field method (FFM), are derived for 3-dimensional fixed-offset GPR imaging of buried objects. The FTM and FFM are obtained by using different asymptotic approximations in the forward model. The two inversion schemes include an accurate electromagnetic description of the GPR antennas through their plane-wave transmitting and receiving spectra. The performance of the FTM is investigated through a numerical example involving a 2.5-dimensional configuration in which the GPR antennas are planar equiangular spiral antennas.**

## I. Introduction

Linear inversion schemes based upon the concept of diffraction tomography (DT) [1] have proven successful for ground penetrating radar (GPR) imaging [2], [3], [4], [5], [6], [7], [8], [9]. On the basis of Devaney's formulation of geophysical DT [10], Witten *et al.* [2], [3] formulated two DT GPR inversion schemes for two-dimensional (2-D) fixed-offset configurations, referred to as the Fourier transform method (FTM) and the far-field method (FFM). The main difference between these two methods is associated with the approximations carried out in the forward model to relate the scattered electric field to the spatial Fourier transform of the object function. In the FTM, the plane-wave (Weyl) expansion of the Green's function for the background medium is inserted into the linearized Lippmann-Schwinger integral equation and an asymptotic evaluation is subsequently carried out to arrive at the above-mentioned relation between the scattered electric field and the object function. In the FFM, the far-field expression of the Green's function for the background medium is used rather than the plane-wave expansion. Since the FTM is based upon plane-wave expansions, it can – as concluded in [3] – be readily implemented using fast Fourier transforms (FFT's), and this method has therefore become more popular than the FFM. In fact, all GPR work within the framework of DT published after the first papers by Witten *et al.* is based on the FTM, including the recent papers by this author [6], [7] in which the FTM is extended to a 3-D fixed-offset GPR configuration and to include the planar air-soil interface. However, in [11], [12] it is shown that the FFM also can be implemented by FFT's, making it as efficient as the FTM. Also, [11], [12] reveal that the FFM is more robust than the FTM when heuristically accounting for the loss in the soil. The forward model of the linear inversion scheme presented by van der Kruk *et al.* [13] for zero-offset GPR is similar to the forward model of the FFM, but the inversion is not DT based.

In the papers mentioned above, except [5], the GPR antennas are assumed to consist of ideal (Hertzian) dipoles [1]. However, the input impedances and the radiation patterns by many GPR antennas – particularly those possessing a phase center with frequency-dependent location – are not accurately described by those of the ideal dipole. It is therefore of interest to derive DT inversion schemes that include electromagnetic descriptions of the GPR antennas.

In this paper the 2.5-dimensional (2.5-D) FTM of [14] is extended to 3-D and the first FFM with antenna models included is derived. The GPR antennas are modeled by using the plane-wave transmitting and receiving spectra of [15]. Throughout the paper the time factor $\exp(-i\omega t)$ is assumed and suppressed.

## II. The Forward Model based on Plane-Wave Spectra of the GPR Antennas

The GPR configuration involving the planar air-soil interface is shown in Figure 1. A Cartesian $xyz$ coordinate system is introduced such that the $xy$ plane coincides with the interface and such that $z > 0$ is air. An object is buried in the soil. The propagation constant of air is $k_0 = \omega\sqrt{\mu_0\varepsilon_0}$ and that of soil is $k_1 = \omega\sqrt{\mu_0\varepsilon_1}$, assuming for simplicity that the soil is lossless. The position of the receiving antenna is described by $\mathbf{r}_r = x_r\hat{\mathbf{x}} + y_r\hat{\mathbf{y}} + z_r\hat{\mathbf{z}}$ and that of the transmitting antenna is $\mathbf{r}_t = x_t\hat{\mathbf{x}} + y_t\hat{\mathbf{y}} + z_t\hat{\mathbf{z}} = \mathbf{r}_r + \mathbf{r}_\Delta$ with the offset $\mathbf{r}_\Delta = x_\Delta\hat{\mathbf{x}} + y_\Delta\hat{\mathbf{y}}$ being fixed. It is assumed that the conductivity $\sigma(x,y,z)$ of the object is much less than the contrast in permittivity $\Delta\varepsilon(x,y,z) = \varepsilon(x,y,z) - \varepsilon_1$, i.e., $\sigma(x,y,z) \ll \omega\Delta\varepsilon(x,y,z)$ over the frequency band $\omega_{\min} \le \omega \le \omega_{\max}$ of interest. Assuming the transmitting antenna is described by the current density $\mathbf{J}_b(x,y,z,\omega)$ when it is located at $(0,0,z_t)$ and fed through a coaxial cable supporting an incident propagating field with voltage $V_b$, the background electric field $\mathbf{E}_b$ in the soil can be

[1] The FTM in [5] formally includes an electromagnetic description of the antennas in terms of their plane-wave transmitting and receiving spectra. However, free-space conditions are assumed and it is therefore not discussed how to obtain the plane-wave spectra when the antennas are close to the air-soil interface.

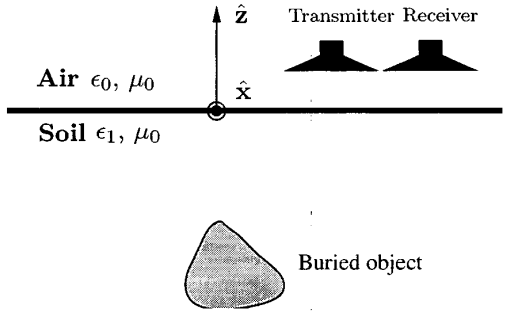


Fig. 1. The fixed-offset GPR configuration involving arbitrary antennas and a buried object.

expressed as [15]

$$\mathbf{E}_b(x',y',z') = \frac{V_b(\omega)}{(2\pi)^2}\int\int_{-\infty}^{\infty}\mathbf{T}_b(k_x,k_y) \cdot\exp(i[k_x(x'-x_t)+k_y(y'-y_t)-\gamma_1 z'])\,dk_x dk_y \tag{1}$$

where the plane-wave transmitting spectrum $\mathbf{T}_b$ is

$$\mathbf{T}_b(k_x,k_y) = \frac{-\omega\mu_0}{2V_b}\bar{\mathbf{F}}(k_x,k_y)\cdot\tilde{\mathbf{J}}_b(k_x,k_y,-\gamma_0). \tag{2}$$

Herein, $\gamma_i = \gamma_i(k_x,k_y) = \sqrt{k_i^2 - k_x^2 - k_y^2}$, $i = 0,1$, and the dyadic $\bar{\mathbf{F}}(k_x,k_y,\omega)$ is given by [6, (6)]. Furthermore, $\tilde{\mathbf{J}}_b$ in (2) is the 3-D spatial Fourier transform of the current density. The multiple interactions between the GPR antenna and the interface are included in the current density $\mathbf{J}_b$ and thus also in the plane-wave spectrum $\mathbf{T}_b$. Assuming that the buried object is a weak scatterer, so that it satisfies the Born approximation, the voltage $V_r$ of the emerging field in the coaxial cable attached to the receiving antenna is

$$V_r(x_r,y_r,\omega) = \frac{i\omega^2\mu_0}{8\pi^2}\int\int_{-\infty}^{\infty}\frac{1}{\gamma_1}\mathbf{R}(k_x,k_y)\iiint_{z'\le 0} \cdot\mathbf{E}_b(x',y',z')\Delta\varepsilon(x',y',z')\exp(i[k_x(x_r-x') +k_y(y_r-y')-\gamma_1 z'])dx'dy'dz'\,dk_x dk_y \tag{3}$$

where $\mathbf{R}$ is the receiving plane-wave spectrum of the antenna. In case of a reciprocal antenna, the receiving spectrum is related to the transmitting spectrum $\mathbf{T}$ of the receiving antenna, defined as in (1), according to [15]

$$\mathbf{R}(k_x,k_y) = \frac{\gamma_1}{\omega\mu_0 Y_c}\mathbf{T}(-k_x,-k_y) \tag{4}$$

where $Y_c$ is the characteristic admittance of the transmission line connected to the receiving antenna.

## III. The Fourier-Transform Method

Replacing $(k_x,k_y)$ with $(k_x',k_y')$ in the expression (1) for $\mathbf{E}_b$ and inserting into (3) for the voltage $V_r$, carrying out the substitutions $k_x = k_x + k_x'$ and $k_y = k_y + k_y'$, and Fourier transforming with respect to $(x_r,y_r)$ yields

$$\tilde{V}_r(k_x,k_y,\omega) = \frac{V_b i\omega^2\mu_0}{8\pi^2}\iiint_{z'<0}\Delta\varepsilon(x',y',z') \cdot\exp(-i[k_x x'+k_y y'])I\,dx'\,dy'\,dz' \tag{5}$$

where $I$ is the integral

$$I = \int\int_{-\infty}^{\infty}H(k_x',k_y')\exp(-iz'[\gamma_1(k_x+k_x', k_y+k_y')+\gamma_1(k_x',k_y')])\,dk_x'\,dk_y' \tag{6}$$

with

$$H(k_x',k_y') = \frac{\mathbf{R}(k_x+k_x',k_y+k_y')\cdot\mathbf{T}_b(k_x',k_y')}{\gamma_1(k_x+k_x',k_y+k_y')} \cdot\exp(-i[k_x'x_\Delta + k_y'y_\Delta]). \tag{7}$$

The integral $I$ can be calculated asymptotically using [6, Appendix] with the result

$$I \sim \frac{i\pi}{k_1 z'}H\left(-\frac{k_x}{2},-\frac{k_y}{2}\right)\left(\gamma_1\left(\frac{k_x}{2},\frac{k_y}{2}\right)\right)^2 \cdot\exp\left(-2iz'\gamma_1\left(\frac{k_x}{2},\frac{k_y}{2}\right)\right) \tag{8}$$

which is accurate when $k_1|z'| \gg 1$. Inserting this asymptotic expression into (3) for $V_r$ the forward model of the FTM becomes

$$\tilde{V}_r(k_x,k_y,\omega) = D_{\text{ftm}}(k_x,k_y,\omega) \cdot\widetilde{\Delta\varepsilon}_1\left(k_x,k_y,\sqrt{4k_1^2-k_x^2-k_y^2}\right) \tag{9}$$

with

$$D_{\text{ftm}}(k_x,k_y,\omega) = \frac{-V_b\omega^2\mu_0}{16\pi k_1}\mathbf{R}\left(\frac{k_x}{2},\frac{k_y}{2}\right) \cdot\mathbf{T}_b\left(-\frac{k_x}{2},-\frac{k_y}{2}\right)\sqrt{4k_1^2-k_x^2-k_y^2} \cdot\exp\left(i\frac{1}{2}[k_x x_\Delta + k_y y_\Delta]\right) \tag{10}$$

and $\Delta\varepsilon_1(x,y,z) = \Delta\varepsilon(x,y,z)/z$.

In DT the forward model (9) is inverted using the inverse Fourier transform. Since $\Delta\varepsilon$ is real, this function can be found from its Fourier transform $\widetilde{\Delta\varepsilon}$ as [6]

$$\Delta\varepsilon(x,y,z) = \frac{1}{4\pi^3}\mathrm{Re}\left[\iiint_{k_z\ge 0}\widetilde{\Delta\varepsilon}(k_x,k_y,k_z) \cdot\exp(i[k_x x+k_y y+k_z z])\,dk_x\,dk_y\,dk_z\right]. \tag{11}$$

To use the relation between measured data $V_r$ and $\widetilde{\Delta\varepsilon}_1$ in the forward model (9), the substitution $k_z = \sqrt{4k_1^2-k_x^2-k_y^2}$ must

be carried out and the integrations over $k_x, k_y$ limited to the region $k_x^2 + k_y^2 < 4k_1^2$ [2]. Hence,

$$\Delta\varepsilon(x,y,z) = \frac{z}{4\pi^3}\mathrm{Re}\left[\int_{\omega_{\min}}^{\omega_{\max}}\iint_{k_x^2+k_y^2<2k_1} \exp(i[k_x x + k_y y + k_z z]) \frac{4k_1\sqrt{\mu_0\varepsilon_1}\,\tilde{V}_r(k_x,k_y,\omega)}{D_{\mathrm{ftm}}(k_x,k_y,\omega)k_z}\,dk_x\,dk_y\,d\omega\right]. \quad (12)$$

## IV. The Far-Field Method

In the FFM, the integrations over $k_x, k_y$ in (1) for $\mathbf{E}_b$ and (3) for $V_r$ are calculated asymptotically before the resulting expression for $\mathbf{E}_b$ is inserted into that for $V_r$. Consider first the double integral in (1). Using the asymptotic approximation of [16, Appendix p. 284], valid as $kR \gg 1$ with $R = \sqrt{(x'-x_t)^2 + (y'-y_t)^2 + z'^2}$, and the usual far-field expansions around a fixed point $\mathbf{r}_0 = x_0\hat{\mathbf{x}} + y_0\hat{\mathbf{y}} + z_0\hat{\mathbf{z}}$ in the soil as well as the center point $\mathbf{r}_c = (\mathbf{r}_r + \mathbf{r}_t)/2$ of the antennas, then $R \approx R_c + \hat{\mathbf{R}}_c \cdot (\mathbf{r}_0 + \frac{\mathbf{r}_\Delta}{2} - \mathbf{r}')$ with $R_c = \sqrt{(x_c-x_0)^2 + (y_c-y_0)^2 + z_0^2}$, $\hat{\mathbf{R}}_c = ((x_c-x_0)\hat{\mathbf{x}} + (y_c-y_0)\hat{\mathbf{y}} - z_0\hat{\mathbf{z}})/R_c$, and $\mathbf{r}' = x'\hat{\mathbf{x}} + y'\hat{\mathbf{y}} + z'\hat{\mathbf{z}}$, and $\mathbf{E}_b$ becomes

$$\mathbf{E}_b \sim \frac{iV_b\mathbf{T}_b(-k_{x0},-k_{y0})k_1 z_0}{2\pi R_c^2}\exp(ik_1R_c) \cdot \exp(ik_1\hat{\mathbf{R}}_c \cdot [\mathbf{r}_0 + \frac{\mathbf{r}_\Delta}{2} - \mathbf{r}']) \quad (13)$$

with

$$k_{x0} = k_1\frac{x_c - x_0}{R_c}, \quad k_{y0} = k_1\frac{y_c - y_0}{R_c}. \quad (14)$$

Second, a similar asymptotic approximation of $V_r$ in (3) yields

$$V_r(x_r,y_r,\omega) \sim \frac{\omega^2\mu_0\exp(ik_1R_c)}{4\pi R_c}\exp(ik_1\hat{\mathbf{R}}_c \cdot [\mathbf{r}_0 - \frac{\mathbf{r}_\Delta}{2}])\mathbf{R}(k_{x0},k_{y0}) \cdot \iiint_{z'<0}\mathbf{E}_b(x',y',z') \cdot \Delta\varepsilon(x',y',z')\exp(-ik_1\hat{\mathbf{R}}_c \cdot \mathbf{r}')\,dx'\,dy'\,dz'. \quad (15)$$

Third, inserting the asymptotic expression (13) for $\mathbf{E}_b$ into (15) above, the forward model of the FFM is obtained,

$$V_r(x_r,y_r,\omega) = D_{\mathrm{ffm}}(x_r,y_r,\omega) \cdot \exp(2ik_1\hat{\mathbf{R}}_c \cdot \mathbf{r}_0)\widetilde{\Delta\varepsilon}(2k_1\hat{\mathbf{R}}_c) \quad (16)$$

where

$$D_{\mathrm{ffm}}(x_r,y_r,\omega) = \frac{iV_b k_1^3 z_0}{8\pi^2 R_c^3\varepsilon_1}\exp(2ik_1R_c) \cdot \mathbf{R}(k_{x0},k_{y0}) \cdot \mathbf{T}_b(-k_{x0},-k_{y0}). \quad (17)$$

This forward model is also inverted using the inverse Fourier transform (11). However, in this case the substitutions $k_j = 2k_1\hat{\mathbf{j}} \cdot \mathbf{R}_c$ with $j = x,y,z$ are employed. Hence, upon setting $\mathbf{r} = \mathbf{r}_0$, the estimate of $\Delta\varepsilon$ becomes

$$\Delta\varepsilon(x_0,y_0,z_0) = \frac{-2z_0(\mu_0\varepsilon_1)^{1.5}}{\pi^3}\mathrm{Re}\left[\int_{\omega_{\min}}^{\omega_{\max}}\int_{y_{\min}}^{y_{\max}}\int_{x_{\min}}^{x_{\max}} \frac{\omega^2 V_r(x_r,y_r,\omega)}{R_c^3 D_{\mathrm{ffm}}(x_r,y_r,\omega)}\,dx_r\,dy_r\,d\omega\right]. \quad (18)$$

This expression can be shown to be in convolutional form and hence, an efficient implementation based on FFT's is possible [11], [12]. Due to the fact that the far-field expansion around the center point $\mathbf{r}_c$ of the antennas is applied, one assumption of the FFM is that $|\mathbf{r}_t - \mathbf{r}_c| \ll R_c$. A version of the FFM not subject to this assumption is derived in [12].

## V. Numerical Example

The FTM presented above is now tested on synthetic 2.5-D GPR data. The zero-offset radar uses 60 frequencies equally spaced in the range 20 MHz $< f <$ 1.3 GHz and the antennas are right-handed self-complementary equiangular planar spiral antennas with expansion ratio 1.87 [17, p. 253], radius 49.4 cm and distance 4 cm above the interface. The buried object is a two-layer dielectric, circular, infinite $\hat{\mathbf{x}}$-directed pipe with outer diameter 24 cm and inner diameter 10 cm located 1 m below the interface. The permittivities of the soil, the inner and outer regions of the pipe are $6\varepsilon_0$, $6.2\varepsilon_0$, and $6.4\varepsilon_0$, respectively. The synthetic GPR data are calculated using the method by Hansen and Meincke [18]. The plane-wave transmitting and receiving spectra of the spiral antenna close to the interface are determined by (2) with the current density of the antennas calculated from the integral equation method in [19]. Figure 2 shows the image of $\Delta\varepsilon(y,z)/\varepsilon_0$ obtained from the 2.5-D version of the FTM in (12). If the usual simple Hertzian dipole antenna model is applied in the inversion, the cylinder is not even visible.

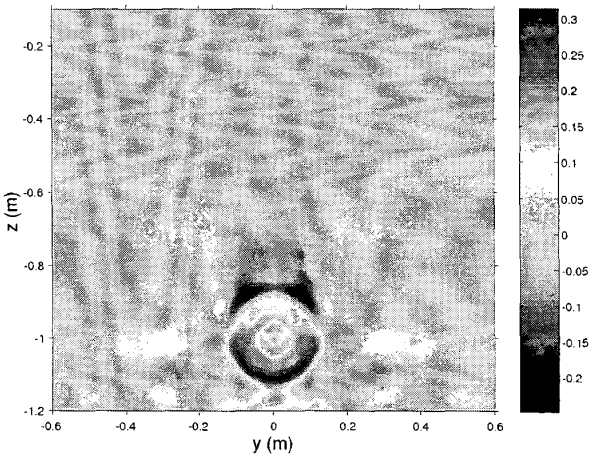


Fig. 2. The image of $\Delta\varepsilon(y,z)/\varepsilon_0$.

[2] The concept of relating data and the object function by using a coordinate transformation constitutes the foundation of the filtered backpropagation algorithm of DT [1].

## ACKNOWLEDGMENT

I thank The Danish Technical Research Council for supporting this work and H.-R. Lenler-Eriksen for generating the method of moment data used in the numerical example.

## REFERENCES

[1] A. J. Devaney, "A filtered backpropagation algorithm for diffraction tomography," *Ultrasonic Imaging*, no. 4, pp. 336–350, 1982.

[2] J. E. Molyneux and A. Witten, "Diffraction tomographic imaging in a monostatic measurement geometry," *IEEE Trans. Geosci. Remote Sensing*, vol. 31, no. 2, pp. 507–511, Mar. 1993.

[3] A. Witten, J. E. Molyneux, and J. E. Nyquist, "Ground penetrating radar tomography: algorithms and case studies," *IEEE Trans. Geosci. Remote Sensing*, vol. 32, no. 2, pp. 461–467, Mar. 1994.

[4] R. Deming and A. J. Devaney, "A filtered backpropagation algorithm for GPR," *J. Environmental and Eng. Geophysics*, no. 2, pp. 113–123, Jan. 1996.

[5] ——, "Diffraction tomography for multi-monostatic ground penetrating radar imaging," *Inverse Problems*, no. 1, pp. 29–45, Feb. 1997.

[6] T. B. Hansen and P. M. Johansen, "Inversion scheme for ground penetrating radar that takes into account the planar air-soil interface," *IEEE Trans. Geosci. Remote Sensing*, vol. 38, pp. 496–506, Jan. 2000.

[7] P. Meincke, "Linear GPR inversion for lossy soil and a planar air-soil interface," *IEEE Trans. Geosci. Remote Sensing*, vol. 39, pp. 2713–2721, Dec. 2001.

[8] T. J. Cui and W. C. Chew, "Diffraction tomography algorithm for the detection of three-dimensional objects buried in a lossy half-space," *IEEE Trans. Antennas Propagat.*, vol. 50, pp. 42–49, Jan. 2002.

[9] S. K. Lehman, "Superresolution planar diffraction tomography through evanescent fields," *Int. Jour. of Imaging Systems and Technology*, no. 1, pp. 16–26, Jan. 2002.

[10] A. J. Devaney, "Geophysical diffraction tomography," *IEEE Trans. Geosci. Remote Sensing*, vol. 22, no. 1, pp. 3–13, Jan. 1984.

[11] P. Meincke, "2.5-D far-field diffraction tomography inversion scheme for GPR that takes into account the planar air-soil interface," in *Proceedings of IEEE Antennas and Propagation Society International Symposium*, Boston, USA, July 2001, pp. 662–665.

[12] ——, "Diffraction tomography inversion scheme for fixed-offset ground penetrating radar using the far-field method," manuscript in preparation.

[13] J. van der Kruk, C. P. A. Wapenaar, J. T. Fokkema, and P. M. van den Berg, "Three-dimensional imaging of multicomponent ground-penetrating radar data," *Geophysics*, vol. 68, pp. 1241–1254, July-August 2003.

[14] P. Meincke and O. S. Kim, "Accurate antenna models in ground penetrating radar diffraction tomography," in *Proceedings of IEEE Antennas and Propagation Society International Symposium*, San Antonio, USA, June 2002, pp. 306–309.

[15] P. Meincke and T. B. Hansen, "Plane-wave characterization of antennas close to a planar interface," *IEEE Trans. Geosci. Remote Sensing*, 2004, to appear.

[16] R. E. Collin, *Antennas and Radiowave Propagation*. New York: McGraw-Hill, 1985.

[17] W. L. Stutzman and G. A. Thiele, *Antenna Theory and Design*. New York: John Wiley & Sons, 1998, 2nd edition.

[18] T. B. Hansen and P. Meincke, "Scattering from a buried circular cylinder illuminated by a 3-D source," *Radio Science*, vol. 37, pp. 4–1 – 4–23, Mar. 2002.

[19] E. Jørgensen, O. S. Kim, P. Meincke, and O. Breinbjerg, "Higher-order hierarchical discretization scheme for surface integral equations for layered media," *IEEE Trans. Geosci. Remote Sensing*, Apr. 2004, to appear.